THERMAL EFFICIENCY OF A COLLECTOR GEOMETRY BASED ON THE ABSORPTION SOLAR COLLECTOR USING OPENFOAM®

Gonçalves, Guilherme Biazzi, guibgoncalves.mec@gmail.com
Scalon, Vicente Luiz, scalon@feb.unesp.br
Padilha, Alcides, padilha@feb.unesp.br
State University of São Paulo (UNESP), Av. Luiz Edmundo Carrijo Coube s/n, Bauru, 17033-360, Brazil

Abstract. *Considering the existing alternative energy sources, solar energy deserves to be highlighted for its great exploitation potential. Solar devices allow a wide range of use and can be implemented in different operations, such as hotels and industries, even in typical home systems. Among the possible applications of solar energy, the commonest one is the Solar Water Heating System (SWHS) using flat plate solar collectors for residences. However, other types of collectors can be used in such systems as the collector geometry based on the direct absorption collector. This paper proposes a new geometry in which the working fluid flows between a black absorber plate, which also heats the fluid, and a glass surface. In order to evaluate the applicability of this collector, a two-dimensional numerical model using OpenFOAM® was prepared in order to determine the thermal efficiency curves in accordance with ISO 9806-1: 1994. So, it was analyzed five distinct fluid thicknesses, ranging between 1.0 mm and 5.0 mm, with different fluid inlet temperature. In addition, it was also evaluated the thickness influence on the bulk temperature in the collector outlet. By analyzing the results, it was concluded that the influence of geometry thickness in the thermal efficiency and bulk temperature is small. Considering the assessed range, the 5.0 mm thickness showed the best values of thermal efficiency and bulk temperature.*

Keywords*: Solar Energy, Solar Collector, Thermal Efficiency, OpenFOAM®*

1. NOMENCLATURE

Symbols
A_a : Absorber Area [m²]
A_c: Total Collector Aperture Area [m²]
c_p: Specific Heat at Constant Pressure [J/kg.K]
F_R: Heat Removal Factor
G_t: Irradiance on Tilted Plane [W/m²]
h: Convection Heat Transfer Coefficient [W/m².K]
k: Thermal Conductivity [W/m.K]
L: Collector's Length [L]
$\dot{m}$: Mass Flow Rate of Fluid [kg/s]
p_h: hydraulic pressure [Pa}
Q_{Rad}: Rate of Radiation Energy Over the Collector [W]
q''_{Rad} : Radiation Flux [W/m²]
Q_u: Rate of Useful Energy Delivered by the Collector [W]
S: Absorbed Solar Radiation per unit of area [J/m²]
T_a: Ambient Temperature [K]
T_i: Inlet Bulk Temperature [K]
T_o: Outlet Bulk Temperature [K]
U_L: Solar Collector Overall Heat Loss Coeficient [W/m².K]
v: Velocity [m/s]
v_w: Wind Velocity [m/s]
Greek
η: Thermal Efficiency
μ: Dynamic Viscosity [N.s/m]
ρ: Density [kg/m³]
$(\tau\alpha)_n$: Transmittance-absorptance product Over the Collector

2. INTRODUCTION

Solar energy is the most abundant renewable resource on the planet and, because of this, it has been subject of numerous studies, in order to increase and improve their exploitation. The main objective of these studies is the usage of the incident solar radiation on Earth's surface, turning it into other forms of energy that can be used by human kind. Despite its huge potential, this kind of technology has high values of manufacturing, installation and maintenance. However, when it is installed, the money and energy savings compensate the initial investment.

Among the forms of solar energy, the commonest one is the Solar Water Heating Systems (SWHS). According Shivakumar (1996), this kind of system is basically consisted by solar collectors and a water tank with internal insulation, which are connected by tubes. The collector is responsible for capturing the sunlight through its upper glass surface, which also helps to reduce the losses by convection and radiation to the environment. Inside the collector, the water can heated directly, when the fluid flows on an absorber plate, or indirectly, when the fluid flows inside tubes. The remaining surfaces are insulated in order to reduce losses by heat transfer. The heated water flows to the tank, where it is stored for use.

One of the collectors that can be used in Solar Water Heating Systems is the Direct Absorption Solar Collector (DASC), also known as volumetric collector. This collector is constituted by an insulated box covered by a glass plate, so the working fluid flows direct inside the collector. Normally, this collector operates with nanofluids, which are mixtures of water and metal nanoparticles, having as main characteristic a greater absorptive capacity of the solar rays in comparison with conventional fluids, resulting in more efficient systems.

However, the nanofluids are expensive and obligate the SWHS to operate by indirect exchange in the storage tank, which increases its installation costs. Thus, the use of water as working fluid is an alternative that can enable the use of DASC with a lower price. In order to make it possible, it needs to be incorporated inside the DASC an absorber plate, so the system will not suffer a significant absorption loss in its capacity.

One of the most practical ways to evaluate mechanism or systems is through a numerical analysis. According Chapra and Canale (2010), this kind of analysis is the study of algorithms in order to solve different types of problems, which aims to design and analyze techniques which provide approximate, however accurate, solutions for problems of difficult or impossible analytical solutions.

It is necessary, to perform a numerical analysis, the usage of specific software, which are developed to analyze and solve the desired problems. Among the available software, one that can be named is the OpenFOAM® (Open Field Operations and Manipulation), which is a CFD (Computational Fluid Dynamics) tool. The OpenFOAM® is open source software, which allows its user to change the implemented codes or create new ones to accomplish specific analysis of complex cases.

Based on what was exposed, this study aims to evaluate the thermal efficiency of a solar collector geometry, based on the DASC, for different water thicknesses. In order to perform this study, a two-dimensional numerical model is created on OpenFOAM®.

3. LITERATURE REVIEW

An alternative that has been recently highlighted for Solar Water Heating Systems is the Direct Absorption Solar Collector, which can be used alone with nanofluids or as hybrid schemes in association with photovoltaic collectors. The use of specific nanofluids is a good alternative, since they increase the fluid absorption capacity and, consequently, causes the absorption of solar rays in the fluid layer, and not by an absorber surface. Thus, as the geometry proposed by this study is similar to the DASC, with an absorber plate as the only difference between them, it was made an evaluation of studies focused in this collector. Many of these studies attempt to evaluate experimentally the nanofluids behavior in comparison to conventional fluids, or they seek the optimal characteristics for the nanofluids.

As regards the study of working fluids, Otanicar, Phelan and Golden (2009) conducted an experimental work in which they evaluated the absorptivity capacity of four fluids: water, propylene glycol, ethylene glycol and Therminol® VP-1. The experiment consisted of locking up the fluids in a layer with 1.0 cm thickness between two layers of Spectrosil® and submitted them to solar radiation, measuring which light wavelengths they easier absorb. The results showed that water has absorbed 13% of solar energy, which is a very low amount of absorbed energy in comparison with nanofluids, but it was the greatest value among the analyzed fluids. Based on the results, the authors concluded that a water layer with 1.0 m thickness is needed to absorb 90% of the sun rays.

Other experimental study was conducted by Saidur et al. (2012) in order to demonstrate the nanofluids, made by a mixture of water and aluminum, effects in the DASC operation. In their analysis, the authors compared the pure water and the nanofluid transmissivity. While the pure water is virtually transparent to the visible region of the light spectrum, the addition of nanoparticles reduces the transmissivity in 60% for the same region. Thus, the superiority of nanofluids in relation to other working fluids is proved.

A similar study was conducted by Ladjevardi et al. (2013) using graphite nanoparticles with different diameters, dissolved in water to create nanofluids with different volumetric concentrations. With this proposal, a numerical and an experimental analysis were made to determine the best parameters combinations that results in the greatest collector thermal efficiency and analyzed the solar rays absorptions for pure water and for nanofluids. The study showed that for a thickness of 1.0 mm of fluid, pure water is able to absorb, approximately, 300 W/m² of solar radiation. However, a small addition of graphite nanoparticles, with volume fraction of 0.00001%, improves the fluid absorption to 400 W/m², and higher concentrations are able to get better results.

An application of a collector with similar geometry to that one analyzed in this study was developed by Purshottam and McKinney (2011). In this case, a collector was designed to heat and sterilize the circulating water in a hospital. The developed collector was composed of an inner plate slots, through which water flows, and two covers made by glass, the first one is placed over the inner plate and the second is positioned above the first one, creating a vacuum between there coverings, which provide a high quality thermal insulation. The water has been quickly heated by the direct exposure to sunlight provided by the collector. Other effect of this system emerges from the germicidal properties of UV rays, which are used to sterilize the water.

Therefore, it is clear the advantage of DASC over the conventional collectors considering the aspects of efficiency and absorb energy. However, the technological problem of nanofluid manufacturing and the low thermal absorptivity of other fluids are obstacles to the implementation of this kind of collectors. Thus, it is necessary to make an adaptation on the collector's model, as the one performed by Purshottam and McKinney (2011). In order to compensate the absence of nanoparticles, which increase the working fluid absorptivity, an absorber black plate should be placed inside the collector box, which is proposed by this study. This plate will perform a similar function to the one exercised by the absorber plate of conventional collectors, which increase the amount of absorbed sunlight and improve the collector efficiency, even using different working fluids, such as water.

4. METHODOLOGY

4.1 Numerical Model

The collector geometry proposed by this study, shown in Fig. 1, is constituted by an insulated box, with a black absorber plate in the bottom surface and a glass plate in the upper surface. The water flows in the space between the plates. In this device, the fluid is partially heated by the radiation that pass through the glass; however, it is the heat dissipated from the absorber plate the major source of energy. On the other hand, the fluid loses heat by convection to the environment through the glass.

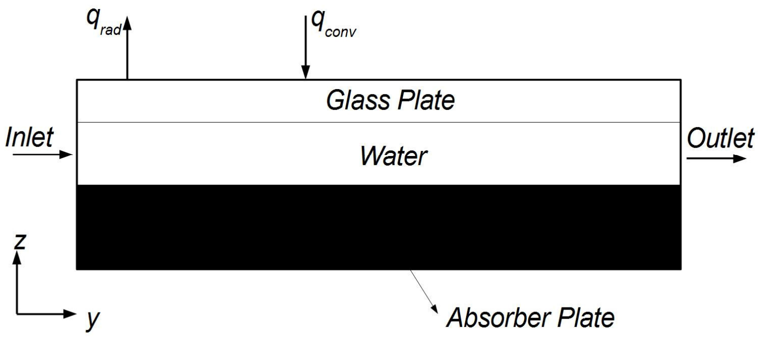

Figure 1. Collector's Analyzed Geometry.

Among the algorithms options present in the OpenFOAM® library, it was chosen to perform the analysis in this study the SIMPLE (Semi-Implicit Method for Pressure Linked Equations) algorithm. According Versteeg and Malalasekera (1995), the algorithm was developed by Patankar and Spalding in 1972 and it's essentially an iterative procedure for calculating the pressure field. In the simulations involving the SIMPLE algorithm, once the system reaches the established tolerance, which is imposed in the solution parameters, it's considered that the steady-state has been reached and the simulation process is stopped.

In order to evaluate the variation of the physical properties of water as the temperature rises, some approximating polynomials, determined from data found in Incropera et al. (2007), were incorporated in the analysis. There were obtained forth order polynomials, which were used to determine the variations of density, Eq. (1), thermal conductivity, Eq. (2), specific heat at constant pressure, Eq. (3), and dynamic viscosity, Eq. (4).

$$\rho = -4.3231 \times 10^{-16} T^4 + 5.58512 \times 10^{-13} T^3 - 0.005T^2 + 2.78T + 611.705 \tag{1}$$

$$k = -5.0 \times 10^{-9} T^4 + 6.47667 \times 10^{-6} T^3 - 0.00315152T^2 + 0.683843T - 55.2758 \tag{2}$$

$$c_p = -4.3231 \times 10^{-15} T^4 + 6.17887 \times 10^{-12} T^3 + 0.01T^2 - 6.26T + 5158.69 \tag{3}$$

$$\mu = 4.757284 \times 10^{-11} T^4 - 6.292028 \times 10^{-8} T^3 + 3.129192 \times 10^{-5} T^2 - 0.006943248T + 0.5810607526 \tag{4}$$

The model created in OpenFOAM® represents the region where the water flows inside the collector and, consequently, has its physical properties. The surfaces were separated according to the imposed boundary conditions, representing: the Inlet (left surface), the Outlet (right surface), the Absorber Plate (bottom surface) and the Glass Cover (upper surface). Additionally, the model has two other surfaces called Walls, which are positioned before the Inlet and after the Outlet. These surfaces are used to allow possible thermal refluxes during the flow without affecting the obtained results, as shown in Fig. 2. The geometry is 1.5 m long (y-direction), which 0.15 m are for each Wall and the 1.2 m are for the collector's area subjected to radiation, 1.0 mm thick (z-direction) and 0.2 mm wide (x-direction).

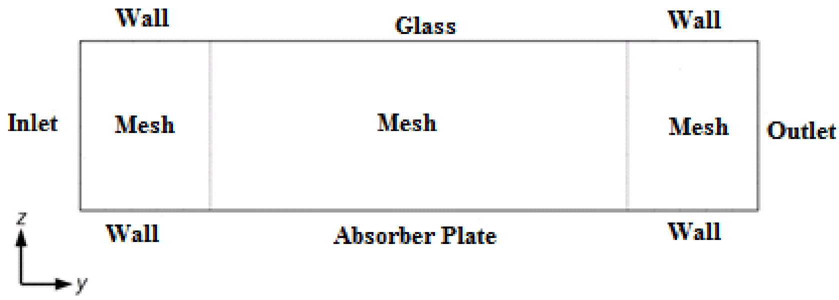

Figure 2. Numerical Model Created in OpenFOAM®.

The model was analyzed considering a constant flow situation entering in the collector with a flow rate by area of 2.0 L/m².min, simulating the condition of pumped water heating system. The boundary conditions used for the static pressure, hydraulic pressure, velocity and temperature fields are shown in Tab. 1. It should be noted that despite the real collector be subjected to a three-dimensional flow, it was considered for this numerical model a symmetry condition on x-axis, which simplifies the simulations for a two-dimensional flow in the yz plane.

Table 1. Boundary Conditions used in the Simulations

Surface	Static Pressure (p)	Hydraulic Pressure (p_rgh)	Velocity (U)	Temperature (T)
Inlet	zeroGradient	fixedFluxPressure	Table 2	Table 3
Outlet	zeroGradient	fixedFluxPressure	zeroGradient	zeroGradient
Glass	zeroGradient	fixedFluxPressure	$v_g = (0\ 0\ 0)\frac{m}{s}$	$\frac{\partial T}{\partial z} = -\left((T - T_a)\left(\frac{h}{k}\right)\right)$
Absorber Plate	zeroGradient	fixedFluxPressure	$v_p = (0\ 0\ 0)\frac{m}{s}$	$q''_{Rad} = 800\frac{W}{m^2}$
Walls	zeroGradient	fixedFluxPressure	$v_w = (0\ 0\ 0)\frac{m}{s}$	zeroGradient
Sidewalls	empty	empty	empty	Empty

As is shown in Tab. 1, a Robin condition was used in the glass surface in order to simulate the convection exchange between the solar collector and the environment. In order to determine the convection losses it's necessary to calculate the convection heat transfer coefficient by the Eq. (5).

$$h = 8.6\frac{v_w^{0.6}}{L^{0.4}} \tag{5}$$

As the model thickness changes in order to determine the thermal efficiency, the inlet velocity needs to change as the thickness change to maintain the flow rate by area of 2.0 L/m².min. The inlet velocities used in this study and the respective thickness correlation are shown in Tab. 2.

Table 2. Relationship between the Thickness and Velocity used in the Simulations

Thickness [mm]	Velocity [m/s]
1.0	0.04
2.0	0.02
3.0	0.013
4.0	0.01
5.0	0.008

Other parameter that was changed during the simulations was the inlet bulk temperature. The values used for this parameter and the reasons why it was varied are shown in the next section.

4.2 Thermal Efficiency of a Collector

With the numerical model defined, the next step of this study was the analysis of the collector's thermal efficiency for five different thicknesses of water, varying from 1.0 mm to 5.0 mm. The calculation is based on the standard for collector's tests ISO 9806-1:1994, which is described in Kalogirou (2009). According to the author and the standard, the thermal efficiency for any type of collector can be obtained by the Eq. (6).

$$\eta = \frac{Q_u}{Q_{Rad}} \rightarrow \eta = \frac{\dot{m} c_p \left(T_o - T_i\right)}{A_a G_t} \tag{6}$$

According Kalogirou (2009), the rate of useful energy (Q_u) can be also estimated considering the heat losses to the environment, as shown in Eq. (7), where the term F_R is described in Eq. (8).

$$Q_u = A_a F_R \left[G_t \left(\tau\alpha\right)_n - U_L \left(T_i - T_a\right) \right] \tag{7}$$

$$F_R = \frac{m c_p \left(T_o - T_i\right)}{A_c \left[S - U_L \left(T_i - T_a\right) \right]} \tag{8}$$

Thus, substituting Eq. (7) in Eq. (6), a new equation for the thermal efficiency for any type of collector is given, as shown in Eq. (8).

$$\eta = F_R \left(\tau\alpha\right)_n - F_R U_L \left(\frac{T_i - T_a}{G_t} \right) \tag{9}$$

During the analysis performed in this study, the only loss incorporated in the model boundary conditions is by convection. Thus, the term U_L present in Eq. (9) can be replaced by the convection heat transfer coefficient h.

For any type of solar collector, there is a relationship between the absorbed solar radiation per unit of area (S) and the irradiance on the plane (G_t), which is shown in Eq. (10).

$$S = \left(\tau\alpha\right)_n G_t \tag{10}$$

In the studied case, the product of transmissivity and incident absorptivity on the collector is assumed to be equal to 1. So, with this hypothesis, which need to be verified in subsequent studies, the Eq. (10) can be substituted by Eq. (11).

$$S = G_t \tag{11}$$

According to the standard, the test for determining the thermal efficiency suggests that the collector needs to be subjected to a series of flows with different inlet temperatures. The lowest temperature must be within a range of ± 3K compared to the ambient temperature and the highest temperature must be equal to the maximum operating temperature of the collector considering the working fluid. For theses simulations, the inlet bulk temperatures used are disposed in Tab. 3. These temperatures were combined with the stipulated thickness, allowing tracing the thermal efficiency graph for each thickness.

Table 3. Inlet Bulk Temperatures used to determine the Thermal Efficiency Curves.

Measurements	Inlet Bulk Temperature [K]
1st Temperature	300
2nd Temperature	313
3rd Temperature	323
4th Temperature	333
5th Temperature	343

5. RESULTS AND DISCUSSION

Some parameters needed to be established in order to perform the simulations. These parameters and their units in the International System are disposed in Tab. 4.

Table 4. Parameters used in the Simulations.

Parameters	Value	Units
Wind Velocity	4.31	[m/s]
Convection Heat Transfer (h)	19.21	[W/m².K]
Gravity Acceleration (g)	9.81	[m/s²]
Environment Temperature (T_a)	300	[K]
Tilt Angle	30	[°]

Before performing the collector's thermal efficiency analysis a mesh size test was done. This test was performed with ten different mesh sizes to select that one which can reproduce the results with good accuracy and time. The results are shown in Fig. 3.

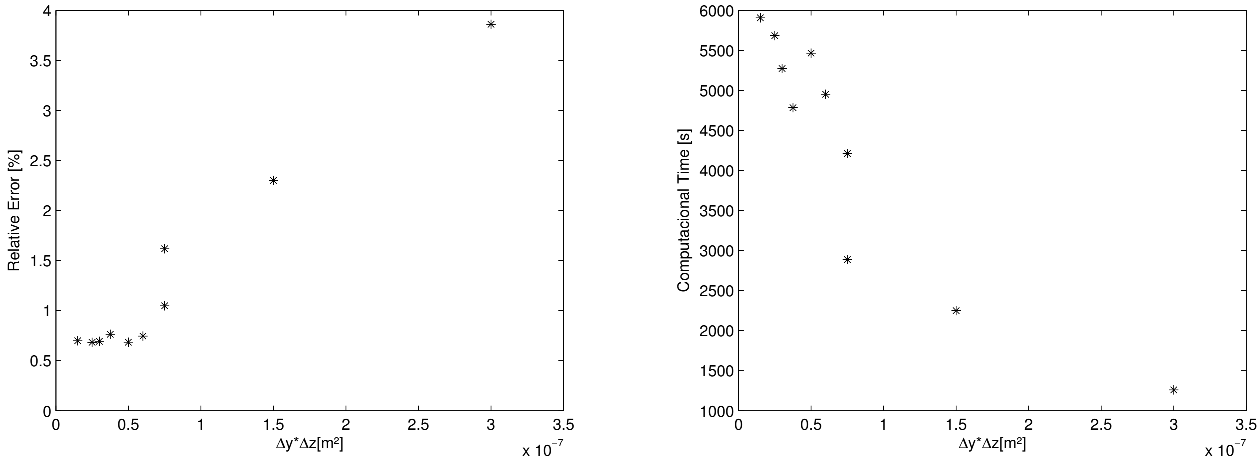

(a) (b)

Figure 3. Results from Mesh Test (a) accuracy (b) elapsed time.

It can be noted by the graphs in Fig. 3 that the lower is the mesh product $\Delta y*\Delta z$, the is the relative error of the simulations results, but it takes more computational time to achieve the specified tolerance. Considering the meshes analyzed, it was chosen the one with the $\Delta y*\Delta z$ ratio equal to $3x10^{-8}$m², because it showed accurate results in an adequate computational time

There were performed 25 simulations combining the thicknesses, from 1.0 mm to 5.0 mm, and the inlet temperatures, from 300 K to 343K. The results were analyzed and used to determine the thermal efficiency curve for thickness using Eq. (6) to Eq. (9). The thermal efficiency curves are disposed in Fig. 4. The outlet bulk temperatures used to determine the efficiency curves are the ones calculated in the end of the geometry that corresponds to the collector area subject to radiation, disregarding the end of the second Wall surface. In order to determine the thermal efficiency curves, it was used the Method of Least Squares to calculate a straight line equation using the values found during the simulations, which resulted in the curves disposed in Fig. 4.

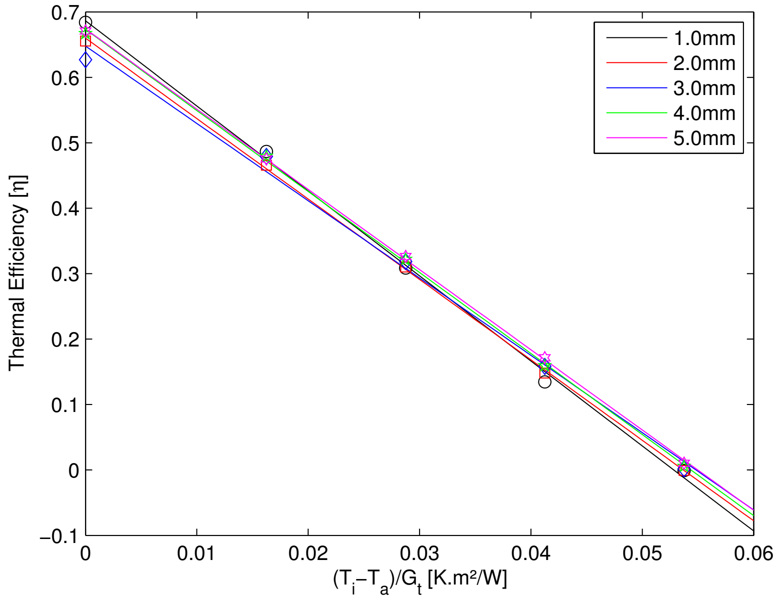

Figure 4. Collector's Thermal Efficiency.

Through the results exposed in Fig. 4, it can be noticed that the thermal efficiencies are similar for the analyzed thicknesses, with small variations from one curve to another. This can be a consequence of the transmissivity and absorptivity hypothesis. Even with this small difference among the curves, the thickness that presented the best thermal efficiencies, in a general way, was 5.0 mm, especially for temperatures higher than 323 K. It can be noticed that as the thickness gets higher, the convection losses to the environment get smaller as the inlet bulk temperatures increase, resulting, consequently, in higher outlet bulk temperatures. For the inlet bulk temperatures nearest to the environment temperature, 300 K and 313 K, the convection losses are smaller, reducing the thickness effects on the outlet bulk temperature. As a consequence, for this range of temperatures, the 1.0 mm thickness showed the best results of thermal efficiency.

It can also be notice in Fig. 4 that some of the thermal efficiencies are negative. This happens because for those geometries, the stagnation temperature was reached. According to Kalogirou (2009), the stagnation temperature of a collector is the temperature at which the heat losses are equal to the gained energy by thermal radiation, resulting in a thermal efficiency equal to zero. Thus, the negative thermal efficiencies mean that the fluid inlet bulk temperature exceeded the collector's stagnation temperature, with more heat losses than gained radiation.

Besides the thermal efficiencies curves, it was also determined some curves for the outlet bulk temperature according to the thickness and the inlet bulk temperature. In order to do this, it was elaborated a similar procedure to the one done for the thermal efficiency using the Method of Least Squares. The curves obtained are represented in Fig. 5.

The curves obtained for the outlet bulk temperature to each thickness are very close. It can be noticed that the same behavior observed for the thermal efficiency curves happens in this case. So, in the simulations that the inlet bulk temperature is close to the environment temperature, 300 K and 313 K, the 1.0 mm thickness showed slight higher outlet bulk temperatures than the other thicknesses and in the other simulations the 5.0 mm thickness obtained the highest values.

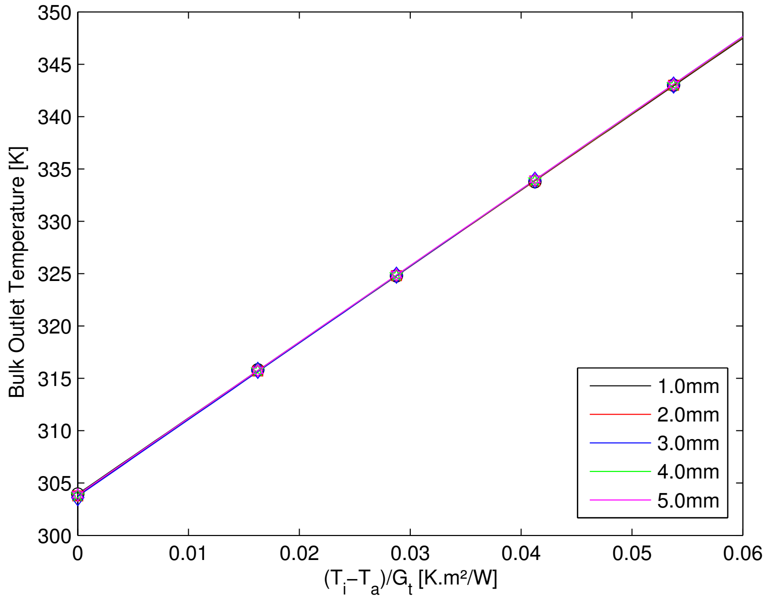

Figure 5. Geometry's Outlet Bulk Temperature.

6. CONCLUSIONS

This study evaluated the thermal efficiency, according Kalogirou (2009) and the standard ISO 9806-1:1994, for five different water thicknesses of a collector's geometry based on the Direct Absorption Solar Collector. In addition, the behavior of the outlet bulk temperature was analyzed for the same thicknesses.

Analyzing the results obtained by the simulations, it can be noticed that the geometry thickness has a small influence on the thermal efficiency and the outlet bulk temperature as the difference between the inlet bulk temperature and ambient temperature increases, with the 5.0 mm thickness presenting the best values among them. It should be noted that for all situations analyzed it was considered that the transmissivity and absorptivity product equal to 1 and the model only loses heat by convection, so other analysis involving different hypothesis for these parameters are necessary to verify if the thermal efficiencies and outlet bulk temperatures have a different behavior then the one showed in this study.

7. REFERENCES

Chapra, S. C. and Canale, R.P., 2010. Numerical Methods for Engineers and Scientists. McGraw Hill, New York.

Incropera, F.P., DeWitt, D.P., Bergman, T.L., Lavine, A.S., 2007. Fundamentals of Heat and Mass Transfer. Wiley, USA.

Kalogirou, S., 2009. Solar Energy Engineering: Processes and Systems". Elsevier, USA.

Ladjervadi, S.M., Asnaghi, A., Izadhast, P.S., Kashani, A.H., 2013. Applicability of graphite nanofluids in direct solar energy absorption. Solar Energy, Vol. 94, pp. 327-334.

Otanicar, T.P., Phelan, P.E., Golden, J.S., 2009. Optical properties of liquids for direct absorption solar thermal energy system. Solar Energy, Vol. 83, pp. 969-977.

Purshottam, P.M. and McKinney, H. 2013. Solar water heater collector for use in hospital, has collector which allows direct absorption solar radiation from sun to produce hot water and sterelize water by germicidal effect of UV radiations from sun. Patent.

Saidur, R., Meng, T.C., Said, Z., Hasanuzzaman, M., Kamyar, A., 2012. Evaluation of the effect of nanofluid-based absorbers on direct solar collector. International Journal of Heat and Mass Transfer, Vol. 55, pp. 5899-5907.

Shivakumar, A. R., 1996. "A value addition to a modern house design: an integrated domestic solar water heater". Energy of Sustainable Development, Vol. 3, nº 1, pp. 54-58.

Versteeg, H.K. and Malalasekera, W., 1995. An Introduction to Computational Fluid Dynamics: The Finite Volume Method. Longman Scientific & Technical, New York.

8. RESPONSIBILITY NOTICE

The authors are the only responsible for the printed material included in this paper.